

Synthesis, Structure, and Dynamic Behavior of Tungsten Dihydride Silyl Complexes $\text{Cp}^*(\text{CO})_2\text{W}(\text{H})_2(\text{SiHPhR})$ ($\text{R} = \text{Ph}, \text{H}, \text{Cl}$)

Hiroyuki Sakaba,* Takeshi Hirata, Chizuko Kabuto, and Kuninobu Kabuto

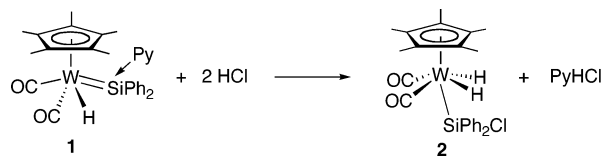
Department of Chemistry, Graduate School of Science, Tohoku University, Aoba-ku, Sendai 980-8578, Japan

Received February 2, 2006

Dihydride silyl complexes $\text{Cp}^*(\text{CO})_2\text{W}(\text{H})_2(\text{SiHPhR})$ ($\text{R} = \text{Ph}$, **7**; H , **8**) were synthesized by treating the donor-stabilized silylene complexes *cis*- $\text{Cp}^*(\text{CO})_2(\text{H})\text{W}=\text{SiRPh}\cdot\text{Do}$ ($\text{R} = \text{Ph}, \text{H}$; $\text{Do} = \text{Py}, \text{THF}$) with LiAlH_4 to give $[\text{Cp}^*(\text{CO})_2\text{W}(\text{H})(\text{SiHPhR})]$ ($\text{R} = \text{Ph}$, **5**; H , **6**) followed by protonation using $\text{CF}_3\text{-COOH}$. X-ray analyses of the crystals of **7** and **8** revealed that the former adopts a distorted pseudo-octahedral structure (**7a**), while the latter possesses a pseudo-trigonal-prismatic structure (**8b**). In solution, both complexes exist as equilibrium mixtures of these two structural isomers: the distorted pseudo-octahedral isomer (**7a/8a**) and the pseudo-trigonal-prismatic isomer (**7b/8b**). In addition to this interconversion process, two dynamic processes involving site exchanges of hydride and silyl ligands in the pseudo-trigonal-prismatic isomer were shown for **8b** by detailed NMR studies. The addition of HCl to *cis*- $\text{Cp}^*(\text{CO})_2(\text{H})\text{W}=\text{SiHPh}\cdot\text{THF}$ afforded $\text{Cp}^*(\text{CO})_2\text{W}(\text{H})_2(\text{SiHPhCl})$ (**9**), which also gave an equilibrium mixture of the distorted pseudo-octahedral isomer (**9a**) and the pseudo-trigonal-prismatic isomer (**9b**). The presence of an additional dynamic process, hydride site exchange in the distorted pseudo-octahedral isomer, was revealed for **9a** due to its chiral silicon center.

Introduction

Recently, much attention has been given to transition metal silyl polyhydride complexes, which display intriguing structural features, such as classical or nonclassical formulation and high fluxionality.¹ For $\text{L}_n\text{MH}_2\text{SiR}_3$ -type complexes, a number of complexes have been characterized for late transition metals such as Ru,² Os,³ Rh,⁴ and Ir.⁵ Especially, recent extensive studies of ruthenium complexes have shown an interesting variation in the formulation: the nonclassical η^2 -silane formulation for $\text{Tp}(\text{Ph}_3\text{P})\text{Ru}(\text{H})(\eta^2\text{-HSiR}_3)$,^{2d} the η^2 -Si–H and SISHA (secondary interactions between silicon and hydrogen atoms) formulation for $\text{RuH}(\eta^2\text{-HSiR}_3)\{\eta^3\text{-C}_6\text{H}_8\}\text{PCy}_2\{\text{PCy}_3\}$,^{2f} the



classical dihydride silyl formulation for $\text{Cp}^*(\text{Ph}_3\text{P})\text{Ru}(\text{H})_2(\text{SiClMe}_2)$,^{2c,g} and the IHI (interligand hypervalent interaction) for $\text{Cp}^*(\text{Pr}_2\text{MeP})\text{Ru}(\text{H})_2(\text{SiClMe}_2)$.^{2g}

In contrast to the rich chemistry of these late transition metal complexes, $\text{L}_n\text{MH}_2\text{SiR}_3$ -type complexes are quite rare for group 6 metals. One such example is the dihydride silyl complex $\text{Cp}^*(\text{CO})_2\text{W}(\text{H})_2(\text{SiPh}_2\text{Cl})$ (**2**), which was obtained in our recent study of the reactivity of the donor-stabilized silylene complex *cis*- $\text{Cp}^*(\text{CO})_2(\text{H})\text{W}=\text{SiPh}_2\cdot\text{Py}$ (**1**) toward HCl.⁶ The HCl adduct **2** adopts a distorted pseudo-octahedral structure with the Cp^* ligand occupying one coordination site at the tungsten in the solid state. The ¹H NMR spectrum of **2** showed a broad hydride signal at room temperature. On decreasing the temperature, the signal became sharp and additional very weak signals appeared in the hydride region. Although this dynamic behavior suggested the existence of the interconversion process of **2** with a trace component, structural information on the latter was unavailable.

(5) For example, see: (a) Fernandez, M. J.; Esteruelas, M. A.; Oro, L. A.; Apreda, M. C.; Foces-Foces, C.; Cano, F. H. *Organometallics* **1987**, *6*, 1751. (b) Rappoli, B. J.; Janik, T. S.; Churchill, M. R.; Thompson, J. S.; Atwood, J. D. *Organometallics* **1988**, *7*, 1939. (c) Hays, M. K.; Eisenberg, R. *Inorg. Chem.* **1991**, *30*, 2623. (d) Esteruelas, M. A.; Nuernberg, O.; Oliván, M.; Oro, L. A.; Werner, H. *Organometallics* **1993**, *12*, 3264. (e) Cleary, B. P.; Mehta, R.; Eisenberg, R. *Organometallics* **1995**, *14*, 2297. (f) Zarate, E. A.; Kennedy, V. O.; McCune, J. A.; Simons, R. S.; Tessier, C. A. *Organometallics* **1995**, *14*, 1802. (g) Chen, W.; Edwards, A. J.; Esteruelas, M. A.; Lahoz, F. J.; Oliván, M.; Oro, L. A. *Organometallics* **1996**, *15*, 2185. (h) Simons, R. S.; Gallucci, J. C.; Tessier, C. A.; Youngs, W. J. *J. Organomet. Chem.* **2002**, *654*, 224. (i) Simons, R. S.; Panzner, M. J.; Tessier, C. A.; Youngs, W. J. *J. Organomet. Chem.* **2003**, *681*, 1.

(6) Sakaba, H.; Hirata, T.; Kabuto, C.; Horino, H. *Chem. Lett.* **2001**, 1078.

* To whom correspondence should be addressed. E-mail: sakaba@funorg.chem.tohoku.ac.jp.

(1) For reviews, see: (a) Schubert, U. *Adv. Organomet. Chem.* **1990**, *30*, 151. (b) Corey, J. Y.; Braddock-Wilking, J. *Chem. Rev.* **1999**, *99*, 175. (c) Kubas, G. J. *Metal Dihydrogen and σ -Bond Complexes: Structure, Theory, and Reactivity*; Kluwer Academic/Plenum Publishers: New York, 2001; Chapter 11. (d) Lin, Z. *Chem. Soc. Rev.* **2002**, *31*, 239.

(2) For example, see: (a) Campion, B. K.; Heyn, R. H.; Tilley, T. D. *Chem. Commun.* **1992**, 1201. (b) Johnson, T. J.; Coan, P. S.; Caulton, K. G. *Inorg. Chem.* **1993**, *32*, 4594. (c) Rodriguez, V.; Donnadieu, B.; Sabo-Etienne, S.; Chaudret, B. *Organometallics* **1998**, *17*, 3809. (d) Ng, S. M.; Lau, C. P.; Fan, M.-F.; Lin, Z. *Organometallics* **1999**, *18*, 2484. (e) Duckett, S. B.; Kuzmina, L. G.; Nikonov, G. I. *Inorg. Chem. Commun.* **2000**, *3*, 126. (f) Lachaize, S.; Sabo-Etienne, S.; Donnadieu, B.; Chaudret, B. *Chem. Commun.* **2003**, 214. (g) Osipov, A. L.; Gerdov, S. M.; Kuzmina, L. G.; Howard, J. A. K.; Nikonov, G. I. *Organometallics* **2005**, *24*, 587.

(3) For example, see: (a) Glaser, P. B.; Tilley, T. D. *Organometallics* **2004**, *23*, 5799. (b) Baya, M.; Crochet, P.; Esteruelas, M. A.; Onate, E. *Organometallics* **2001**, *20*, 240. (c) Maseras, F.; Lledos, A. *Organometallics* **1996**, *154*, 1218. (d) Esteruelas, M. A.; Oro, L. A.; Valero, C. *Organometallics* **1991**, *10*, 462.

(4) For example, see: (a) Osakada, K.; Sarai, S.; Koizumi, T.; Yamamoto, T. *Organometallics* **1997**, *16*, 3973. (b) Osakada, K.; Koizumi, T.; Sarai, S.; Yamamoto, T. *Organometallics* **1998**, *17*, 1868. (c) Noveski, D.; Braun, T.; Schulte, M.; Neumann, B.; Stammler, H.-G. *Dalton Trans.* **2003**, 4075. (d) Turculet, L.; Feldman, J. D.; Tilley, T. D. *Organometallics* **2004**, *23*, 2488. (e) Taw, F. L.; Bergman, R. G.; Brookhart, M. *Organometallics* **2004**, *23*, 886. (f) Cook, K. S.; Incarvito, C. D.; Webster, C. E.; Fan, Y.; Hall, M. B.; Hartwig, J. F. *Angew. Chem., Int. Ed.* **2004**, *43*, 5474.

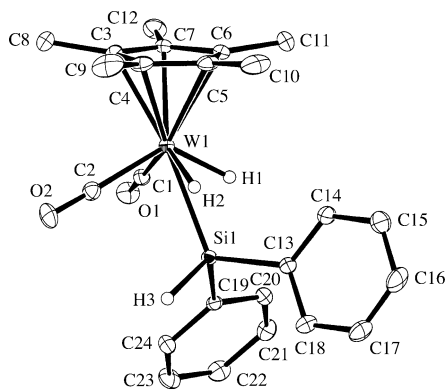
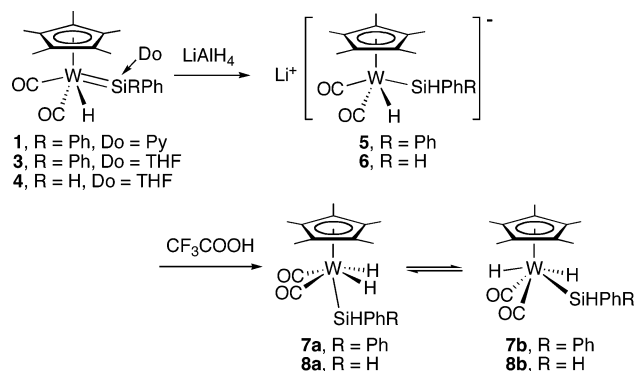


Figure 1. ORTEP drawing of **7a**. Methyl and phenyl hydrogen atoms are omitted for clarity. Selected bond distances (Å) and angles (deg): W(1)–Si(1) 2.5798(7), W(1)–C(1) 2.012(2), W(1)–C(2) 1.989(2), W(1)–H(1) 1.77(4), W(1)–H(2) 1.66(4), Si(1)–C(13) 1.900(2), Si(1)–C(19) 1.885(2), Si(1)–H(3) 1.45(3), C(1)–O(1) 1.134(3), C(2)–O(2) 1.143(3); Si(1)–W(1)–C(1) 81.88(8), Si(1)–W(1)–C(2) 78.16(8), Si(1)–W(1)–H(1) 50.6(15), Si(1)–W(1)–H(2) 47.8(11), C(1)–W(1)–C(2) 84.92(10), C(1)–W(1)–H(1) 75.9(15), C(2)–W(1)–H(2) 76.3(13), H(1)–W(1)–H(2) 78.3(19).

Scheme 1



In further studies of structurally related complexes $\text{Cp}^*(\text{CO})_2\text{W}(\text{H})_2(\text{SiHPhR})$ (R = Ph, **7**; H, **8**; Cl, **9**), we found a rare example of equilibrium between distorted pseudo-octahedral and pseudo-trigonal-prismatic isomers of $\text{CpL}_2\text{M}(\text{H})_2(\text{SiR}_3)$ -type complexes, shedding light on the unresolved dynamic behavior of **2**. In addition, three dynamic processes involving site exchanges of hydride and silyl ligands in these isomers were revealed by detailed variable-temperature ^1H NMR studies. Here, we describe the structure, isomerism, and dynamic behavior of $\text{Cp}^*(\text{CO})_2\text{W}(\text{H})_2(\text{SiHPhR})$ complexes.

Results and Discussion

Protonation using CF_3COOH of the lithium tungstate $\text{Li}[\text{Cp}^*(\text{CO})_2\text{W}(\text{H})(\text{SiHPh}_2)]$ (**5**), which was prepared by the reaction of *cis*- $\text{Cp}^*(\text{CO})_2(\text{H})\text{W}=\text{SiPh}_2\cdot\text{Do}$ (Do = pyridine, **1**; THF, **3**) with LiAlH_4 ,⁶ afforded $\text{Cp}^*(\text{CO})_2\text{W}(\text{H})_2(\text{SiHPh}_2)$ (**7**) as air-sensitive yellow crystals in 54% yield after recrystallization from hexane at -60°C (Scheme 1).

X-ray analysis of the yellow crystals showed the distorted pseudo-octahedral structure **7a** (Figure 1, Table 1). Two hydrides are located nearly symmetrically with respect to the plane defined by the W1 and Si1 atoms and the centroid (CNT) of the Cp^* ligand. The W1–Si1 bond is bent by $26.5(1)^\circ$ away from the CNT–W1 vector toward the hydrides. A similar structure has been found for **2**.⁶ The W1–H1 (1.77(4) Å) and

Table 1. Crystal Data for **7a** and **8b**

	7a	8b
formula	$\text{C}_{24}\text{H}_{28}\text{O}_2\text{SiW}$	$\text{C}_{18}\text{H}_{24}\text{O}_2\text{SiW}$
fw	560.42	484.32
cryst syst	triclinic	monoclinic
space group	$P\bar{1}$ (No. 2)	$P2_1/n$ (No. 14)
color	yellow	yellow
Z	2	4
a, Å	10.086(3)	8.5362(18)
b, Å	10.642(3)	15.006(3)
c, Å	11.511(3)	14.409(3)
α , deg	74.631(9)	
β , deg	87.934(11)	91.597(4) ^o
γ , deg	76.153(9)	
V, Å ³	1156.2(5)	1845.0(7)
D_{calcd} , g/cm ³	1.610	1.743
T, K	173	173
R1 ($I > 2\sigma(I)$)	0.0207	0.0244
wR2 (all data)	0.0580	0.0670
GOF	1.027	1.111

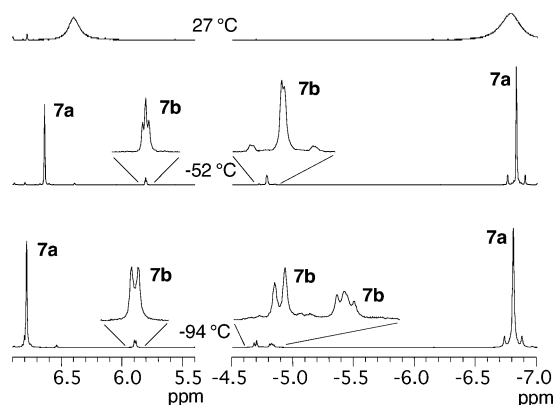


Figure 2. Variable-temperature ^1H NMR spectra of **7** in toluene- d_8 showing SiH signals (left) and WH signals (right).

W1–H2 (1.66(4) Å) lengths are comparable to the W–H bond lengths in the X-ray structures of CpWHL_3 -type complexes.⁷ Although it is difficult to determine accurately the positions of hydrogens bound to heavy atoms by X-ray analysis, the H1···H2 separation of 2.17(5) Å would exclude the possibility of an $\eta^2\text{-H}_2$ coordination. This is supported by a $T_1(\text{min})$ value of 540 ms at -50°C (400 MHz) for the hydride signal (vide infra for spectral characterization). The Si1···H1 and Si1···H2 distances of 2.00(4) and 1.91(3) Å, respectively, are longer than typical $\eta^2\text{-Si-H}$ bond distances (1.6–1.8 Å)^{1c} and are at the boundary between silyl(hydrido) and $\eta^2\text{-Si-H}$ coordination. Considering that substantial silyl–hydrido interaction has been suggested for Si···H distances up to 2.1 Å,^{1d} there may be some interactions in the WSiH_2 moiety, although it is difficult to evaluate interactions by X-ray data.

The ^1H NMR spectrum of a toluene- d_8 solution of the crystalline **7** showed broad SiH (δ 6.40) and WH (δ –6.79) signals at room temperature (Figure 2). A decrease in temperature led to their decoalescence to give two sets of SiH and WH signals: δ 6.64 (s, 1H, $J_{\text{SiH}} = 198$ Hz) and –6.83 (s, 2H, $J_{\text{WH}} = 58$ Hz, $J_{\text{SiH}} = 16$ Hz) for the major isomer and δ 5.80 (t, 1H, $J_{\text{HH}} = 2.7$ Hz, $J_{\text{SiH}} = 193$ Hz) and –4.78 (d, 2H, $J_{\text{HH}} = 2.7$ Hz, $J_{\text{WH}} = 52$ Hz) for the minor isomer in a ratio of 89:11 at -52°C . Interestingly, on further cooling to -94°C , the

(7) For example, see: (a) Baker, R. T.; Calabrese, J. C.; Harlow, R. L.; Williams, I. D. *Organometallics* **1993**, *12*, 830. (b) Malisch, W.; Hirth, U.-A.; Grun, K.; Schmeusser, M.; Fey, O.; Weis, U. *Angew. Chem., Int. Ed. Engl.* **1995**, *34*, 2500.

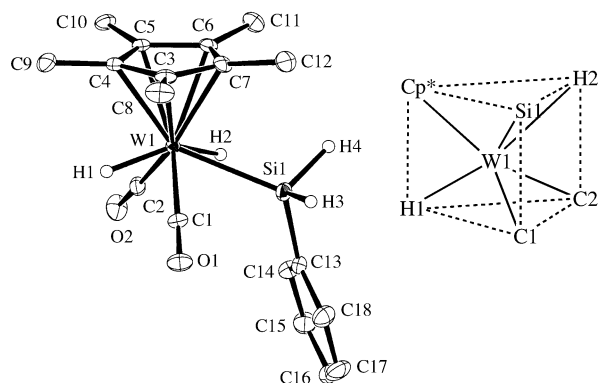


Figure 3. ORTEP drawing of **8b** with a schematic representation of pseudo-trigonal-prismatic structure. Methyl and phenyl hydrogen atoms are omitted for clarity. Selected bond distances (Å) and angles (deg): W(1)–Si(1) 2.5691(10), W(1)–C(1) 1.973(3), W(1)–C(2) 1.986(3), W(1)–H(1) 1.66(5), W(1)–H(2) 1.71(4), Si(1)–C(13) 1.874(3), Si(1)–H(3) 1.42(4), Si(1)–H(4) 1.41(5), C(1)–O(1) 1.145(4), C(2)–O(2) 1.149(4); Si(1)–W(1)–C(1) 67.68(11), Si(1)–W(1)–H(2) 51.7(15), C(1)–W(1)–H(1) 67.0(17), C(2)–W(1)–H(1) 73.2(17), C(2)–W(1)–H(2) 63.0(13).

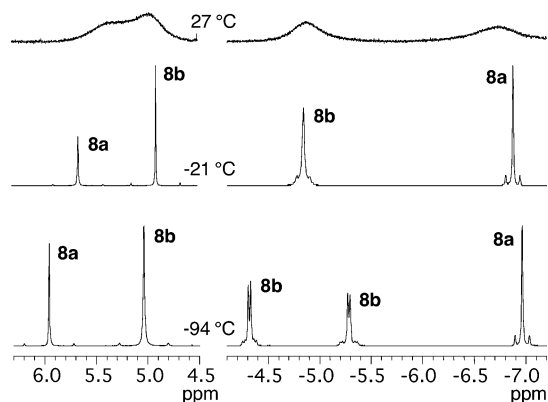


Figure 4. Variable-temperature ^1H NMR spectra of **8** in toluene- d_8 showing SiH signals (left) and WH signals (right).

hydride signal of the minor isomer was split into an AB-type signal at δ -4.82 (dd, $J = 8.6, 5.4$ Hz) and -4.69 (d, $J = 8.6$ Hz) for the ABX system involving a SiH doublet signal (δ 5.89, $J = 5.4$ Hz) as the X part, while no such signal splitting was seen for the hydride of the major isomer. The major isomer is assigned to **7a**, and the minor isomer is characterized as the pseudo-trigonal-prismatic complex **7b** from the spectral characteristics and with the help of the structure determination of the corresponding monophenyl derivative **8b** (vide infra). These spectral changes indicate that **7a** is in equilibrium with **7b** and that a rapid dynamic process averages the inequivalent hydride signals of **7b**.

Protonation of $\text{Li}[\text{Cp}^*(\text{CO})_2\text{W}(\text{H})(\text{SiH}_2\text{Ph})]$ (**6**) obtained by treating *cis*- $\text{Cp}^*(\text{CO})_2(\text{H})\text{W}=\text{SiHPh}\cdot\text{THF}$ (**4**) with LiAlH_4 gave $\text{Cp}^*(\text{CO})_2\text{W}(\text{H})_2(\text{SiH}_2\text{Ph})$ (**8**) as pale yellow crystals in 50% yield after recrystallization from pentane at -60 °C (Scheme 1). The X-ray crystal analysis revealed a rare example of a pseudo-trigonal-prismatic half-sandwich CpML_5 structure, **8b** (Figure 3, Table 1). To our knowledge, the only previous example of this type of structure determined by X-ray analysis is $\text{Cp}^*\text{MoH}_3(\text{dppe})$, reported by Poli.^{8a,b} In **8b**, one triangular face is defined by one of the hydrides (H1) and two carbonyl carbons (C1 and C2), and the other triangular face is defined by the $\text{Cp}^*(\text{CNT})$, Si1, and second hydride (H2). With respect

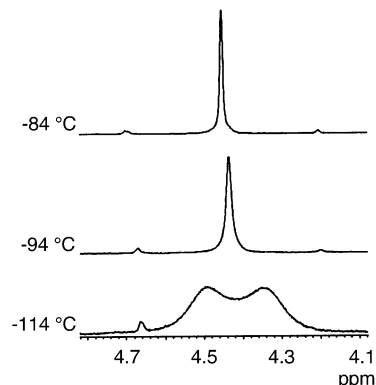
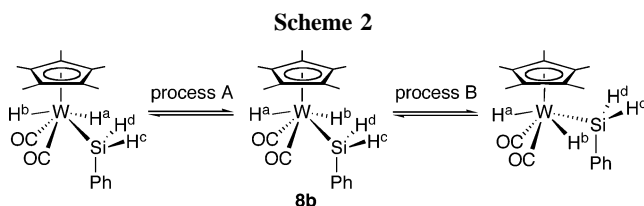


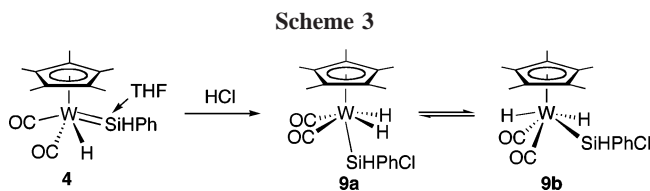
Figure 5. Variable-temperature ^1H NMR spectra of **8b** in $\text{THF-}d_8$ showing SiH signals.



to the CNT-W1-H1 plane, the two CO ligands are located fairly symmetrically, as shown by the bond angles of $\text{C1-W1-H1} = 67(2)^\circ$ and $\text{C2-W1-H1} = 73(2)^\circ$, and the silyl and hydride (H2) ligands are also coordinated symmetrically: $\text{H2-W1-CNT} = 113.5(1)^\circ$ and $\text{Si1-W1-CNT} = 112.5(1)^\circ$. The W1-H1 and W1-H2 bond lengths are 1.66(5) and 1.71(4) Å, respectively. The $\text{Si1}\cdots\text{H2}$ distance of 2.02(4) Å is also at the boundary between silyl(hydrido) and η^2 -silane coordination, similar to the case of **7a**.

Variable ^1H NMR spectra of **8** in toluene- d_8 also showed the existence of two isomers, as shown in Figure 4. At room temperature, two very broad SiH signals were observed near δ 5.35 and 4.98, along with two broad WH signals at δ -4.87 and -6.73 , and these signals became sharp upon cooling to -21 °C: δ 4.90 (s, 2H, $J_{\text{SiH}} = 190$ Hz) and -4.84 (br s, 2H, $J_{\text{WH}} = 49$ Hz) for the major isomer and δ 5.66 (s, 2H, $J_{\text{SiH}} = 194$ Hz) and -6.87 (s, 2H, $J_{\text{WH}} = 56$ Hz) for the minor isomer. The WH signal at δ -4.84 (major) was further split into two doublets at δ -4.32 (1H, $J_{\text{HH}} = 9.1$ Hz, $J_{\text{WH}} = 43$ Hz) and -5.28 (1H, $J_{\text{HH}} = 9.1$ Hz, $J_{\text{WH}} = 57$ Hz) at -94 °C, while the signal at δ -6.87 (minor) remained a singlet, showing spectral changes similar to those observed for **7a,b**. The major isomer affording the two WH signals is assigned to **8b**, where two inequivalent signals are expected for the diastereotopic SiH protons (H^c and H^d in Scheme 2) in a slow-exchange limiting spectrum. At -94 °C in $\text{THF-}d_8$, the SiH signal of **8b** was still observed as a slightly broad singlet, but further lowering to -114 °C led to the expected decoalescence, giving two broad SiH signals at δ 4.35 and 4.49 (Figure 5). This behavior indicates the existence of an extremely rapid process equalizing the diastereotopic SiH signals. The minor isomer giving a single WH signal is characterized as **8a** on the basis of the similarity of its spectral characteristics to **7a**, including the $T_1(\text{min})$ values (400 MHz) of their hydrides: 540 ms at -50 °C for **7a** and 550 ms at -60 °C for **8a**. The hydride signal of **8a** was observed

(8) (a) Fettinger, J. C.; Pleune, B. A.; Poli, R. *J. Am. Chem. Soc.* **1996**, *118*, 4906. (b) Pleune, B.; Poli, R.; Fettinger, J. C. *Organometallics* **1997**, *16*, 1581. (c) Abugideiri, F.; Fettinger, J. C.; Pleune, B.; Poli, R.; Bayse, C. A.; Hall, M. B. *Organometallics* **1997**, *16*, 1179.



as a singlet down to $-114\text{ }^\circ\text{C}$ in $\text{THF-}d_8$, showing no sign of decoalescence. Thus, we observed three dynamic processes for **8**: the equilibrium between **8a** and **8b** (Scheme 1), the averaging process of the hydride signals in **8b** (process A in Scheme 2), and that of the diastereotopic SiH signals (enantiomer interconversion, process B). For these processes, the following activation parameters were obtained from variable-temperature ^1H NMR spectra and their simulations: $\Delta H^\ddagger = 13.5 \pm 0.7\text{ kcal mol}^{-1}$ and $\Delta S^\ddagger = -1.1 \pm 1.7\text{ eu}$ for **8a** to **8b** in toluene- d_8 , $\Delta H^\ddagger = 9.8 \pm 0.6\text{ kcal mol}^{-1}$ and $\Delta S^\ddagger = 0.3 \pm 2.1\text{ eu}$ for the process A in toluene- d_8 , and $\Delta H^\ddagger = 8.0 \pm 0.9\text{ kcal mol}^{-1}$ and $\Delta S^\ddagger = 3.1 \pm 3.8\text{ eu}$ for the process B in $\text{THF-}d_8$.⁹ These activation entropies are close to zero, in accordance with intramolecular processes.

To investigate the possibility of hydride site exchange in the distorted pseudo-octahedral isomer, $\text{Cp}^*(\text{CO})_2\text{W}(\text{H})_2(\text{SiHPhCl})$ (**9**), having a chiral silicon center, was synthesized by the reaction of **4** with HCl (Scheme 3). Even though this exchange process exists in **7a** and **8a**, it cannot be observed, as these complexes lack the chiral center. The ^1H NMR spectrum of **9** in $\text{THF-}d_8$ at $20\text{ }^\circ\text{C}$ showed broad SiH and WH signals at δ 6.78 and -6.67 , respectively (Figure 6). When the temperature was decreased, these signals were split into two sets of signals assigned to **9a** (major) and **9b** (minor). At $-21\text{ }^\circ\text{C}$, **9a** showed sharp SiH and WH signals at δ 6.86 (1H) and -6.87 (2H), respectively, while **9b** gave very broad SiH and WH signals at δ 6.16 (1H) and -5.01 (2H), respectively. At $-84\text{ }^\circ\text{C}$, the WH signal of **9b** decoalesced into two signals at δ -4.05 (d, $J = \text{ca. } 8.0\text{ Hz}$) and -6.14 , and the SiH signal was observed as a triplet at δ 6.12 ($J = \text{ca. } 3.5\text{ Hz}$). These spectral changes for **9b** are explained by a slowing of hydride site exchange, as seen for **8b**. Importantly, a hydride signal due to **9a** at δ -7.06 broadened at $-84\text{ }^\circ\text{C}$ and split into two signals at δ -6.54 and -7.73 at $-114\text{ }^\circ\text{C}$, which demonstrates the existence of the hydride site exchange in the distorted pseudo-octahedral isomer. For this process, $\Delta H^\ddagger = 8.1 \pm 0.6\text{ kcal mol}^{-1}$ and $\Delta S^\ddagger = 3.2 \pm 2.4\text{ eu}$ were estimated by spectral simulation.⁹

Interconversion between the pseudo-trigonal-prismatic isomer and the pseudo-octahedral isomer has been proposed for the fluxional behaviors of $[\text{Cp}^*\text{Mo}(\text{H})_{3-n}(\text{MeCN})_n(\text{dppe})]^{n+}$ ($n = 0, 1, 2$) and $\text{Cp}^*\text{Mo}(\text{H})_3(\text{PMe}_2\text{Ph})_2$, where the former structure has been determined for $\text{Cp}^*\text{Mo}(\text{H})_3(\text{dppe})$ and the latter structure for $[\text{Cp}^*\text{Mo}(\text{H})(\text{MeCN})_2(\text{dppe})]^{2+}$ and $\text{Cp}^*\text{Mo}(\text{H})_3(\text{PMe}_2\text{Ph})_2$ by X-ray analyses.⁸ Interestingly, in our $\text{Cp}^*(\text{CO})_2\text{W}(\text{H})_2(\text{SiR}_3)$ system, simple variation of the substituents on the silyl ligand allowed us to determine both types of structures and to reveal clearly the details of the dynamic processes as shown above.

The equilibrium between the distorted pseudo-octahedral isomers **7a–9a** and the pseudo-trigonal-prismatic isomers **7b–9b** is shifted toward the former by substitution of a hydrogen atom at the silyl group of **8** with bulky and electronegative substituents, as shown by isomeric ratios of **9a:9b** (SiHPhCl) = 94:6, **7a:7b** (SiHPh_2) = 89:11, and **8a:8b** (SiH_2Ph) = 37:63 at $-51\text{ }^\circ\text{C}$, shedding light on understanding the previous

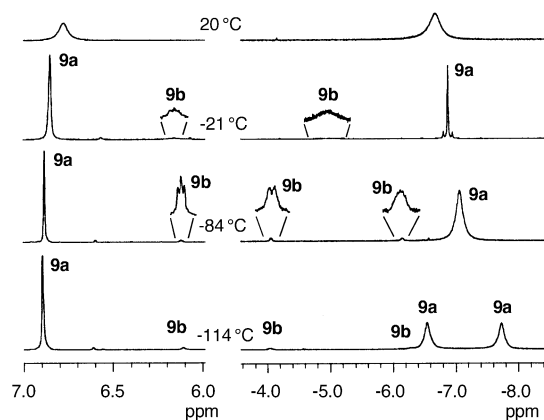


Figure 6. Variable-temperature ^1H NMR spectra of **9** in $\text{THF-}d_8$ showing SiH signals (left) and WH signals (right).

unresolved observation for **2**.⁶ A further increase in the bulkiness of the SiPh_2Cl group in **2** compared to **9** is expected to favor the distorted pseudo-octahedral isomer to reduce the pseudo-trigonal-prismatic isomer to a trace level, suggesting that the trace component may be assignable to the pseudo-trigonal-prismatic isomer of **2**.

In summary, the dihydride silyl complexes $\text{Cp}^*(\text{CO})_2\text{W}(\text{H})_2(\text{SiHPhR})$ ($\text{R} = \text{Ph}$, **7**; H , **8**; Cl , **9**) were synthesized from the donor-stabilized silylene complexes $\text{cis-Cp}^*(\text{CO})_2(\text{H})\text{W}=\text{SiRPh}$. Do and revealed the solid-state and solution structures of their two structural isomers: distorted pseudo-octahedral isomers **7a–9a** and pseudo-trigonal-prismatic isomers **7b–9b**. Variable-temperature NMR studies also revealed the details of four dynamic processes in the isomers, i.e., (1) the equilibrium between distorted pseudo-octahedral isomer **8a** and pseudo-trigonal-prismatic isomer **8b** (Scheme 1), (2) the averaging process of the hydride signals in **8b** (process A in Scheme 2), (3) the averaging process of the diastereotopic SiH signals in **8b** (process B in Scheme 2), and (4) the hydride site exchange in distorted pseudo-octahedral isomer **9a**. The activation barriers for the four processes decrease in the order (1) > (2) > (3) \approx (4). Further theoretical studies are needed to elucidate fully the mechanisms of these dynamic processes and the degree of Si \cdots H interactions in these complexes. A pseudo-Bailar twist mechanism has been proposed for the fluxional processes of $\text{Cp}^*\text{Mo}(\text{H})_3(\text{dppe})$ and related complexes.⁸

Experimental Section

General Methods. All reactions and procedures were carried out under an atmosphere of nitrogen using standard glovebox, Schlenk, and high-vacuum-line techniques. Photolyses were carried out using an Ushio UM-103 100 W medium-pressure Hg lamp placed in a water-cooled Pyrex jacket. NMR spectra were recorded on a JEOL JNM-GSX400 (^1H , 399.7 MHz; ^{13}C , 100.4 MHz; ^{29}Si , 79.3 MHz) spectrometer. IR spectra were obtained on a Shimadzu FTIR-8100M spectrometer. Mass spectra were recorded on a JEOL HX-110 mass spectrometer, and X-ray crystal analyses were performed using a Rigaku/MSC Mercury CCD diffractometer at the Instrumental Analysis Center for Chemistry, Tohoku University.

Diethyl ether, hexane, tetrahydrofuran, toluene, tetrahydrofuran- d_8 , and toluene- d_8 were distilled from sodium benzophenone ketyl. $\text{Cp}^*(\text{CO})_3\text{WMe}$ was prepared according to the literature methods.¹⁰ LiAlH_4 (1.0 M solution in Et_2O , Aldrich) was used as received. Ph_2SiH_2 (Tokyo Kasei) and PhSiH_3 (Tokyo Kasei) were stored over

(9) For details, see Supporting Information.

(10) Mahmoud, K. A.; Rest, A. J.; Alt, H. G.; Eichner, M. E.; Jansen, B. M. *J. Chem. Soc., Dalton Trans.* **1984**, 175.

4 Å molecular sieves under a nitrogen atmosphere. CF₃COOH (Aldrich) was degassed and vacuum transferred immediately prior to use.

cis-Cp*(CO)₂(H)W=SiPh₂·THF (3). A solution of Cp*(CO)₃WMe (806 mg, 1.93 mmol) and Ph₂SiH₂ (0.7 mL, 4 mmol) in THF (30 mL) was irradiated for 50 min with a 100 W medium-pressure Hg lamp. After removal of the solvent, the residue was washed with hexane (8 mL) to give a pale yellow powder of **3** (836 mg, 1.33 mmol, 69%). The sample for elemental analysis was recrystallized from THF. Upon dissolving **3** in THF-*d*₈, the coordinated THF is replaced by THF-*d*₈ to give **3-d**₈ and free THF. ¹H NMR (400 MHz, THF-*d*₈): δ -9.20 (s, *J*_{WH} = 68.8 Hz, 1H, WH), 1.77 (m, 4H, free THF), 1.94 (s, 15H, Cp*), 3.62 (m, 4H, free THF), 7.23–7.31 (m, 6H, Ph), 7.49 (dd, *J* = 8.1, 1.6 Hz, 4H, Ph). ¹³C{¹H} NMR (100 MHz, THF-*d*₈): δ 11.7 (C₅Me₅), 26.3 (free THF), 68.2 (free THF), 100.7 (C₅Me₅), 128.1 (Ph), 128.9 (Ph), 135.6 (Ph), 146.4 (Ph (ipso)), 234.8 (CO, *J*_{WC} = 161.2 Hz). ²⁹Si{¹H} NMR (79 MHz, THF-*d*₈): δ 119.3 (*J*_{WSi} = 103.3 Hz). IR (THF): 1896 (s, ν_{CO}), 1809 (m, ν_{CO}) cm⁻¹. Anal. Calcd for C₂₈H₃₄O₃SiW: C, 53.34; H, 5.44. Found: C, 53.49; H, 5.90.

cis-Cp*(CO)₂(H)W=SiHPh·THF (4). A solution of Cp*(CO)₃WMe (805 mg, 1.93 mmol) and PhSiH₃ (0.9 mL, 7 mmol) in THF (15 mL) was irradiated for 55 min with a 100 W medium-pressure Hg lamp. After removal of the solvent, the residue was washed with hexane (10 mL) to give a pale yellow powder of **4** (747 mg, 1.35 mmol, 70%). The sample for elemental analysis was recrystallized from THF. Upon dissolving **4** in THF-*d*₈, the coordinated THF is replaced by THF-*d*₈ to give **4-d**₈ and free THF. ¹H NMR (400 MHz, THF-*d*₈): δ -9.91 (d, ³*J*_{HH} = 4.3 Hz, *J*_{WH} = 67.7 Hz, 1H, WH), 1.78 (m, 4H, free THF), 2.12 (s, 15H, Cp*), 3.62 (m, 4H, free THF), 7.23 (d, ³*J*_{HH} = 4.3 Hz, *J*_{SiH} = 178.4 Hz, 1H, SiH), 7.2–7.3 (m, 3H, Ph), 7.66 (dd, *J* = 8.1, 2.1 Hz, 2H, Ph). ¹³C{¹H} NMR (100 MHz, THF-*d*₈): δ 11.9 (C₅Me₅), 26.3 (free THF), 68.2 (free THF), 100.7 (C₅Me₅), 128.2 (Ph), 129.5 (Ph), 136.4 (Ph), 145.9 (Ph (ipso)), 234.4 (CO, *J*_{WC} = 160.2 Hz). ²⁹Si{¹H} NMR (79 MHz, THF-*d*₈): δ 117.1 (*J*_{WSi} = 109.9 Hz). IR (THF): 1900 (s, ν_{CO}), 1813 (s, ν_{CO}) cm⁻¹. Anal. Calcd for C₂₂H₃₀O₃SiW: C, 47.66; H, 5.45. Found: C, 47.54; H, 5.43.

Li[Cp*(CO)₂W(H)(SiHPh₂)] (5). A flask was charged with *cis*-Cp*(CO)₂(H)W=SiPh₂·THF (**3**) (836 mg, 1.33 mmol) in the glovebox. On the vacuum line, Et₂O (5 mL) was added via vacuum transfer at -196 °C. At this temperature, LiAlH₄ (1.0 M solution in Et₂O, 1.4 mL, 1.4 mmol) was added via syringe under a nitrogen atmosphere. The solution was stirred at -60 °C for 3 min and then at room temperature for 7 min. The resulting pale yellow solid was filtered through a glass frit, washed with small amounts of Et₂O, and dried in vacuo to give **5** (756 mg, 1.33 mmol, 100%). ¹H NMR (400 MHz, THF-*d*₈): δ -7.18 (s, *J*_{WH} = 74.1 Hz, 1H, WH), 1.92 (s, 15H, Cp*), 5.35 (d, *J*_{SiH} = 159.6 Hz, 1H, SiH), 6.93 (t, *J* = 7.5 Hz, 2H, Ph), 7.01 (t, *J* = 7.5 Hz, 4H, Ph), 7.65 (d, *J* = 7.5 Hz, 4H, Ph). ¹³C{¹H} NMR (100 MHz, THF-*d*₈): δ 11.9 (C₅Me₅), 99.7 (C₅Me₅), 126.3 (Ph), 126.8 (Ph), 137.1 (Ph), 150.9 (Ph (ipso)), 241.2 (CO, *J*_{WC} = 169.9 Hz). ²⁹Si{¹H} NMR (79 MHz, THF-*d*₈): δ 29.4 (*J*_{WSi} = 71.7 Hz). IR (THF): 1867 (s, ν_{CO}), 1717 (s, ν_{CO}) cm⁻¹.

Li[Cp*(CO)₂W(H)(SiH₂Ph)] (6). A flask was charged with *cis*-Cp*(CO)₂(H)W=SiHPh·THF (**4**) (466 mg, 0.841 mmol) in the glovebox. On the vacuum line, Et₂O (10 mL) was added via vacuum transfer at -196 °C. At this temperature, LiAlH₄ (1.0 M solution in Et₂O, 0.86 mL, 0.86 mmol) was added via syringe under a nitrogen atmosphere. The solution was stirred at -60 °C for 4 min and then at room temperature for 15 min. Methanol (2.6 mmol) was added via vacuum transfer at -196 °C to quench any unreacted LiAlH₄. After the mixture was stirred at room temperature for 4 min, the solvent was removed in vacuo. The residue was extracted with Et₂O (4 × 6 mL), and the extracts were filtered through glass fiber filter paper. After removal of the solvent, the residual yellow solid was washed with pentane (2 mL) and dried in vacuo to give

6 (373 mg, 0.761 mmol, 90%). ¹H NMR (400 MHz, THF-*d*₈): δ -7.57 (s, *J*_{WH} = 73.6 Hz, 1H, WH), 2.02 (s, 15H, Cp*), 4.64 (s, *J*_{SiH} = 159.0 Hz, 2H, SiH), 6.96 (t, *J* = 7.5 Hz, 1H, Ph), 7.03 (t, *J* = 7.5 Hz, 2H, Ph), 7.66 (d, *J* = 7.5 Hz, 2H, Ph). ¹³C{¹H} NMR (100 MHz, THF-*d*₈): δ 11.8 (C₅Me₅), 99.2 (C₅Me₅), 126.3 (Ph), 126.7 (Ph), 137.4 (Ph), 148.2 (Ph (ipso)), 241.1 (CO, *J*_{WC} = 168.8 Hz). ²⁹Si{¹H} NMR (79 MHz, THF-*d*₈): δ -6.9 (*J*_{WSi} = 71.0 Hz). IR (THF): 1867 (s, ν_{CO}), 1717 (s, ν_{CO}) cm⁻¹.

Cp*(CO)₂W(H)₂(SiHPh₂) (7). A flask was charged with Li-[Cp*(CO)₂W(H)(SiHPh₂)] (**5**) (236 mg, 0.417 mmol) in the glovebox. On the vacuum line, toluene (6 mL) and CF₃COOH (0.46 mmol) were added via vacuum transfer at -196 °C. The mixture was stirred at -60 °C for 8 min. The solvent was removed, and the residue was extracted with hexane (4 × 6 mL). The extracts were filtered through glass fiber filter paper. After removal of the solvent, the residue was recrystallized from hexane at -60 °C to give yellow crystals of **7** (126 mg, 0.225 mmol, 54%). ¹H NMR (400 MHz, toluene-*d*₈, 27 °C): δ -6.79 (br, 2H, WH, **7a** + **7b**), 1.79 (s, 15H, Cp*, **7a** + **7b**), 6.40 (br, 1H, SiH, **7a** + **7b**), 7.12 (t, *J* = 7.5 Hz, 2H, Ph, **7a** + **7b**), 7.22 (t, *J* = 7.5 Hz, 4H, Ph, **7a** + **7b**), 7.79 (d, *J* = 7.5 Hz, 4H, Ph, **7a** + **7b**). ¹H NMR (400 MHz, toluene-*d*₈, -94 °C): δ -6.80 (s, *J*_{WH} = 57.2 Hz, 2H, WH, **7a**), -4.82 (dd, *J* = 8.6, 5.4 Hz, 1H, WH, **7b**), -4.69 (d, *J* = 8.6 Hz, WH, **7b**), 1.53 (s, 15H, Cp*, **7b**), 1.63 (s, 15H, Cp*, **7a**), 5.89 (s, *J* = 5.4 Hz, 1H, SiH, **7b**), 5.90 (s, *J*_{SiH} = 196.6 Hz, 1H, SiH, **7a**), 7.07–7.23 (m, 6H, Ph, **7b**), 7.18 (t, *J* = 7.0 Hz, 2H, Ph, **7a**), 7.31 (t, *J* = 7.0 Hz, 4H, Ph, **7a**), 7.94 (d, *J* = 7.0 Hz, 2H, Ph, **7a**), 8.00 (d, *J* = 7.0 Hz, 2H, Ph, **7b**). ¹³C{¹H} NMR (100 MHz, toluene-*d*₈, -60 °C): δ 10.8 (C₅Me₅, **7b**), 11.2 (C₅Me₅, **7a**), 100.3 (C₅Me₅, **7a**), 102.2 (C₅Me₅, **7b**), 135.3 (Ph, **7a**), 135.8 (Ph, **7b**), 140.9 (Ph (ipso), **7b**), 145.0 (Ph (ipso), **7a**), 212.3 (CO, *J*_{WC} = 134.2 Hz, **7b**), 224.7 (CO, *J*_{WC} = 147.2 Hz, **7a**). ²⁹Si{¹H} NMR (79 MHz, toluene-*d*₈, -60 °C): δ -6.5 (*J*_{WSi} = 5.8 Hz, **7a**), 14.3 (*J*_{WSi} = 22.8 Hz, **7b**). IR (toluene): 2062 (w, ν_{SiH}), 1991 (s, ν_{CO}), 1976 (sh, ν_{CO}), 1927 (s, ν_{CO}), 1898 (w, ν_{CO}), ca. 1860 (br, w, ν_{WH}) cm⁻¹. Anal. Calcd for C₂₄H₂₈O₂SiW: C, 51.44; H, 5.04. Found: C, 51.28; H, 5.07.

Cp*(CO)₂W(H)₂(SiH₂Ph) (8). A flask was charged with Li-[Cp*(CO)₂W(H)(SiH₂Ph)] (**6**) (228 mg, 0.465 mmol) in the glovebox. On the vacuum line, toluene (6 mL) and CF₃COOH (0.51 mmol) were added via vacuum transfer at -196 °C. The mixture was stirred at -60 °C for 8 min. The solvent was removed in vacuo, and the residue was extracted with hexane (5 × 5 mL). The extracts were filtered through glass fiber filter paper. After removal of the solvent, the residual solid was recrystallized from pentane at -60 °C to give yellow crystals of **8** (113 mg, 0.233 mmol, 50%). ¹H NMR (400 MHz, toluene-*d*₈, 27 °C): δ -6.73 (br, 2H, WH, **8a**), -4.87 (br, 2H, WH, **8b**), 1.78 (s, 15H, Cp*, **8a** + **8b**), 5.16 (br, 2H, SiH, **8a** + **8b**), 7.13 (t, *J* = 7.5 Hz, 1H, Ph, **8a** + **8b**), 7.22 (t, *J* = 7.5 Hz, 2H, Ph, **8a** + **8b**), 7.83 (dd, *J* = 8.1, 1.1 Hz, 2H, Ph, **8a** + **8b**). ¹H NMR (400 MHz, toluene-*d*₈, -94 °C): δ -6.96 (s, *J*_{WH} = 56.1 Hz, 2H, WH, **8a**), -5.28 (d, *J*_{HH} = 9.1 Hz, *J*_{WH} = 57.1 Hz, 1H, WH, **8b**), -4.32 (d, *J*_{HH} = 9.1 Hz, *J*_{WH} = 43.1 Hz, 1H, WH, **8b**), 1.59 (s, 15H, Cp*, **8a**), 1.62 (s, 15H, Cp*, **8b**), 5.04 (s, *J*_{SiH} = 189.7 Hz, 2H, SiH, **8b**), 5.96 (s, *J*_{SiH} = 191.5 Hz, 2H, SiH, **8a**), 7.09 (t, *J* = 7.5 Hz, 1H, Ph, **8b**), 7.24 (t, *J* = 7.5 Hz, 2H, Ph, **8b**), 7.27 (t, *J* = 7.5 Hz, 1H, Ph, **8a**), 7.38 (t, *J* = 7.5 Hz, 2H, Ph, **8a**), 8.01 (d, *J* = 7.5 Hz, 2H, Ph, **8a**), 8.09 (d, *J* = 7.5 Hz, 2H, Ph, **8b**). ¹H NMR (400 MHz, THF-*d*₈, -114 °C): δ -7.31 (s, *J*_{WH} = 55.5 Hz, 2H, WH, **8a**), -5.67 (d, ²*J*_{HH} = 9.2 Hz, *J*_{WH} = 57.1 Hz, 1H, WH, **8b**), -4.66 (d, ²*J*_{HH} = 9.2 Hz, *J*_{WH} = 43.1 Hz, 1H, WH, **8b**), 2.22 (s, 15H, Cp*, **8b**), 2.31 (s, 15H, Cp*, **8a**), 4.35 (br, 1H, SiH, **8b**), 4.49 (br, 1H, SiH, **8b**), 4.90 (s, *J*_{SiH} = 188.7 Hz, 2H, SiH, **8a**), 7.32–7.38 (m, 3H, Ph, **8a** + **8b**), 7.52 (m, 1H, Ph, **8a** + **8b**), 7.62 (m, 1H, Ph, **8a** + **8b**). ¹³C{¹H} NMR (100 MHz, toluene-*d*₈, -80 °C): δ 10.4 (C₅Me₅, **8b**), 11.0 (C₅Me₅, **8a**), 100.1 (C₅Me₅, **8a**), 101.8 (C₅Me₅, **8b**), 135.8 (Ph, **8a**), 136.0 (Ph, **8b**), 211.1

(CO, $J_{WC} = 132.0$ Hz, **8b**), 224.1 (CO, $J_{WC} = 145.0$ Hz, **8a**). $^{13}\text{C}\{-^1\text{H}\}$ NMR (100 MHz, THF- d_8 , -114 °C): δ 10.8 (C_5Me_5 , **8b**), 11.6 (C_5Me_5 , **8a**), 101.9 (C_5Me_5 , **8a**), 103.2 (C_5Me_5 , **8b**), 128.3 (Ph, **8a**), 128.5 (Ph, **8b**), 129.2 (Ph, **8a**), 129.7 (Ph, **8b**), 136.0 (Ph, **8a**), 136.1 (Ph, **8b**), 138.5 (Ph, **8b**), 141.8 (Ph, **8a**), 211.6 (br, $J_{WC} = 129.9$ Hz, CO, **8b**), 224.8 ($J_{WC} = 146.1$ Hz, CO, **8a**). $^{29}\text{Si}\{^1\text{H}\}$ NMR (79 MHz, toluene- d_8 , -80 °C): δ -31.9 (**8a**), -17.2 ($J_{\text{WSi}} = 23.7$ Hz, **8b**). IR (toluene): 2074 (w, ν_{SiH}), 1990 (sh, ν_{CO}), 1979 (s, ν_{CO}), 1929 (m, ν_{CO}), 1902 (s, ν_{CO}), ca. 1855 (br, w, ν_{WH}) cm^{-1} . Anal. Calcd for $\text{C}_{18}\text{H}_{24}\text{O}_2\text{SiW}$: C, 44.64; H, 4.99. Found: C, 44.55; H, 5.09.

Cp*(CO)₂W(H)₂(SiHPhCl) (9). A flask was charged with *cis*-Cp*(CO)₂(H)W=SiHPh·THF (**4**) (454 mg, 0.819 mmol) in the glovebox. On the vacuum line, THF (7 mL) and HCl (0.90 mmol) were added via vacuum transfer at -196 °C. The mixture was allowed to warm to room temperature and stirred for 15 min. After removal of the solvent and washing with hexane (5 mL), the residue was recrystallized from toluene/hexane (3 mL/3.5 mL) at -20 °C to give yellow crystals of **9** (325 mg, 0.626 mmol, 77%). ^1H NMR (400 MHz, THF- d_8 , 20 °C): δ -6.67 (br, 2H, WH, **9a** + **9b**), 2.25 (s, 15H, Cp*, **9a** + **9b**), 6.78 (br, 1H, SiH, **9a** + **9b**), 7.23–7.35 (m, Ph, **9a** + **9b**), 7.64–7.70 (m, Ph, **9a** + **9b**). ^1H NMR (THF- d_8 , -84 °C): δ -7.06 (br, 2H, WH, **9a**), -6.14 (br, 1H, WH, **9b**), -4.05 (d, $J_{\text{HH}} = \text{ca. } 8.0$ Hz, 1H, WH, **9b**), 2.27 (s, 15H, Cp*, **9b**), 2.30 (s, 15H, Cp*, **9a**), 6.12 (t, $J_{\text{HH}} = \text{ca. } 3.5$ Hz, 1H, SiH, **9b**), 6.88 (s, $J_{\text{SiH}} = 224$ Hz, 1H, SiH, **9a**), 7.10–7.25 (m, 3H, Ph, **9b**), 7.32–7.43 (m, 3H, Ph, **9a**), 7.60 (d, $J_{\text{HH}} = 7$ Hz, 2H, Ph, **9b**), 7.68 (d, $J_{\text{HH}} = 7$ Hz, 2H, Ph, **9a**). $^{13}\text{C}\{^1\text{H}\}$ NMR (toluene- d_8 , -60 °C): δ 10.7 (C_5Me_5 , **9b**), 10.8 (C_5Me_5 , **9a**), 100.9 (C_5Me_5 , **9a**), 103.7

(C_5Me_5 , **9b**), 127.9 (Ph, **9a**), 129.4 (Ph, **9a**), 134.4 (Ph, **9a**), 146.6 (Ph, **9a**), 221.2 (CO, $J_{WC} = 142.8$ Hz, **9a**), 221.9 (CO, $J_{WC} = 147.2$ Hz, **9a**). $^{29}\text{Si}\{^1\text{H}\}$ NMR (toluene- d_8 , -80 °C): δ 11.3 ($J_{\text{WSi}} = 5.1$ Hz, **9a**), 37.6 ($J_{\text{WSi}} = 33.6$ Hz, **9b**). Anal. Calcd for $\text{C}_{18}\text{H}_{23}\text{ClO}_2\text{SiW}$: C, 41.68; H, 4.47. Found: C, 41.92; H, 4.52.

Variable-Temperature NMR Studies and Dynamic NMR Simulations. The temperature of the NMR probe was calibrated with methanol. Line shape analyses were carried out using the gNMR program version 4.1 (Cherwell Scientific). The rates as a function of temperature were determined by visual comparison of the experimental and simulated spectra. The activation parameters were calculated from the Eyring equations by using a linear least-squares procedure, and the errors were computed from error propagation formulas.¹¹

X-ray Crystal Structure Determination. Single crystals of **7a** and **8b** were obtained by recrystallization at -60 °C from hexane and pentane, respectively. All measurements were made on a Rigaku Mercury CCD area detector with graphite-monochromated Mo K α radiation ($\lambda = 0.71070$ Å). The data were corrected for Lorentz and polarization effects. The structures were solved by the direct method (SIR92)¹² and expanded using difference Fourier techniques (DIRDIF99).¹³ The refinement was carried out using full-matrix least-squares method on F^2 . All non-hydrogen atoms were refined anisotropically, and the hydrogen atoms of the Cp* and Ph groups were calculated and refined with a riding model. Tungsten and silicon hydrides were located in the difference map and refined isotropically. Atomic scattering factors were taken from International Tables for X-ray Crystallography.¹⁴ All calculations were performed using the CrystalStructure crystallographic software package.¹⁵

Acknowledgment. This work was supported by a Grant-in-Aid for Scientific Research from the Ministry of Education, Culture, Sports, Science and Technology, Japan.

Supporting Information Available: Experimental and simulated variable-temperature NMR spectra for complexes **7–9** (PDF). X-ray crystallographic data for **7a** and **8b** (PDF, CIF). This material is available free of charge via the Internet at <http://pubs.acs.org>.

OM060101R

(11) Morse, P. M.; Spencer, M. D.; Wilson, S. R.; Girolami, G. S. *Organometallics* **1994**, *13*, 1646.

(12) Altomare, A.; Cascarano, G.; Giacovazzo, C.; Guagliardi, A.; Burla, M.; Polidori, G.; Camalli, M. *J. Appl. Crystallogr.* **1994**, *27*, 435.

(13) Beurskens, P. T.; Admiraal, G.; Beurskens, G.; Bosman, W. P.; de Gelder, R.; Israel, R.; Smits, J. M. M. *The DIRDIF-99 program system*; Technical Report of the Crystallography Laboratory; University of Nijmegen: The Netherlands, 1999.

(14) Cromer, D. T.; Waber, J. T. *International Tables for X-ray Crystallography*; Kynoch Press: Birmingham, UK, 1974; Vol IV.

(15) *CrystalStructure 3.7, Crystal Structure Analysis Package*; Rigaku and Rigaku/MSK, 2000–2005.